

SU(N) Quantum Spin Models: A Variational Wavefunction Study

Arun Paramakanti

Department of Physics, University of Toronto, Toronto, Ontario M5S-1A7 CANADA

E-mail: arunp@physics.utoronto.ca

J. B. Marston

Department of Physics, Box 1843, Brown University, Providence, RI 02912-1843 USA

E-mail: marston@physics.brown.edu

Abstract. SU(N) quantum spin systems may be realized in a variety of physical systems including ultracold atoms in optical lattices. The study of such models also leads to insights into possible novel quantum phases and phase transitions of SU(2) spin models. Here we use Gutzwiller projected fermionic variational wavefunctions to explore the phase diagram and correlation functions of SU(N) quantum spin models in the self-conjugate representation. In one dimension, the ground state of the SU(4) spin chain with Heisenberg bilinear and biquadratic interactions is studied by examining instabilities of the Gutzwiller projected free fermion ground state to various broken symmetries. The variational phase diagram so obtained agrees well with exact results. The spin-spin and dimer-dimer correlation functions of the Gutzwiller projected free fermion state with N flavors of fermions are in good agreement with exact and 1/N calculations for the critical points of SU(N) spin chains. In two dimensions, the phase diagram of the antiferromagnetic Heisenberg model on the square lattice is obtained by finding instabilities of the Gutzwiller projected flux state. In the absence of biquadratic interactions the model exhibits long range Neel order for N = 2 and 4, and spin Peierls (columnar dimer) order for N > 4. Upon including biquadratic interactions in the SU(4) model (with sign appropriate to a fermionic Hubbard model), the Neel order diminishes and eventually disappears, giving way to an extended valence bond crystal. In the case of the SU(6) model, the dimerized ground state melts at sufficiently large biquadratic interaction yielding to a projected flux spin liquid phase which in turn undergoes a transition into an extended valence bond crystal at even larger biquadratic interaction. The spin correlations of the projected flux state at N = 4 are in good agreement with 1/N calculations. We find that the state shows strongly enhanced dimer correlations, in qualitative agreement with recent theoretical predictions. We also compare our results with a recent quantum Monte Carlo study of the SU(4) Heisenberg model.

PACS numbers: 75.50.Ee, 75.10.Jm, 71.10.Fd

1. Introduction

Quantum spin models provide a setting in which one can explore interesting strong correlation physics that arises from quantum fluctuations. Such fluctuations can be large enough, in certain cases, to melt any form of classical order leading to various exotic spin liquid states[1, 2]. A class of spin liquids of particular interest are those that support gapless excitations. Apart from experimental questions regarding their possible existence [3, 4, 5, 6, 7], it is interesting to inquire under what circumstances such gapless spin liquids can arise in two or more dimensions. The Bethe ansatz solution of the spin-1/2 Heisenberg antiferromagnet chain is a well-known exact example of such a gapless spin-liquid in one spatial dimension, but much less is known about higher dimensions. This question was raised in the early days of high- T_c theory, as Anderson's original proposal for a resonating valence bond (RVB) spin liquid had a Fermi surface of gapless spinon excitations[8, 9].

One route to accessing the physics of some of these spin disordered states is by generalizing the usual SU(2) spin models to SU(N) models. As N increases from 2 to larger values, quantum spin fluctuations are enhanced, weakening any spin order. Such models can accommodate several types of spontaneously broken symmetries: Spin order, spin dimerization, and charge-conjugation symmetry breaking[10]. We note that models of SU(N) quantum spins are not purely theoretical exercises: It may be possible to realize them with ultracold atoms in optical lattices[11, 12, 13], in quantum dot arrays[14], or as special points in models with spin and orbital degrees of freedom [15], although the effects of SU(N) symmetry breaking terms need to be carefully examined in each case.

Of the many possible representations of SU(N), we focus on a particular self-conjugate representation with $N=2$ fermions on each site, each with a different flavor due to the Pauli exclusion principle[16, 17]. In this representation, the generators of the SU(N) algebra may be expressed in terms of the fermion creation and annihilation operators as: $S_i = \frac{1}{2} f_i^\dagger f_i$. The constraint $S_i = 0$ thus holds in the subspace with exactly $N=2$ fermions on each site, and consequently there are the correct number $(N^2 - 1)$ of special unitary generators. The representation is called "self-conjugate" because upon making a particle-hole transformation the same representation, namely one with $N=2$ fermions, is obtained. All representations of SU(2), regardless of the total spin, are automatically self-conjugate, but only certain representations of SU($N > 2$) are self-conjugate. An advantage of the self-conjugate representation is that it is easy to construct SU(N) invariant Hamiltonians that retain all of the symmetries of the underlying lattice, and hence mimic SU(2) models in this regard. For more details, including the Young tableau classification, see reference [10].

In the $N \rightarrow \infty$ limit saddle point solutions of the fermionic path integral are exact and the operator constraint $S_i = 0$ constraint can be replaced by the much simpler mean-field constraint $\langle S_i \rangle = 0$. These large-N SU(N) antiferromagnets cannot break global SU(N) spin symmetry; some possess ground states that do not

break any lattice symmetry and thus furnish mean field caricatures of a class of spin liquids. Going from $N = 1$ down to the physical limit of $N = 2$ requires the inclusion of fluctuations about the mean field state, and the problem can be recast in the form of a strongly coupled gauge theory interacting with fermionic matter fields. Progress toward calculating the properties of such a field theory relies on a $1/N$ expansion, and some results have been obtained in this manner for one and two dimensional models [18, 19, 20, 21, 22, 23, 24, 25, 26, 27, 28, 29, 30, 31, 32] though not without controversy. There is also good reason to be concerned about the reliability of such an expansion in the physically important SU(2) case as N is of course no longer large. DMRG calculations for SU(N) quantum antiferromagnets [14] and Hubbard models [33] provide some confirmation of analytical understanding of one-dimensional (1D) chains. In two dimensions (2D) there is a very interesting quantum Monte Carlo (QMC) study of SU(N) quantum antiferromagnets by Aissaad [34] that we discuss further in section 3.

A different approach to the study of SU(N) spin models also begins with mean field states that satisfy the average constraint $\langle S_i \rangle = 0$, but then the operator constraint $S_i^2 = 0$ is implemented via an on-site Gutzwiller projection. The Gutzwiller projection operator forces the number of fermions to be precisely $N=2$ at each site. For $N = 2$, and denoting as usual the two spin states by \uparrow, \downarrow , the projection operator takes the well-known form $P_G = \prod_i (1 - n_{i\uparrow}n_{i\downarrow})$. The resulting many-body wavefunction thus lives in the correct Hilbert space for SU(N) antiferromagnets and serves as a variational approximation to the spin ground state. For $N = 1$, a probabilistic central limit argument shows that the Gutzwiller projection is unimportant and gives the same result as the mean field state. For any finite N , projection is crucial and nontrivial; the advantage of the approach is that the projection constraint can be handled numerically exactly with the variational Monte Carlo algorithm. Thus the generalization to SU(N) provides a rationale for understanding the Gutzwiller procedure: Mean-field wavefunctions obtained in the large- N limit are then modified by projection to account for the occupancy constraint at finite N . The approach however suffers from the criticism that it is biased and restricted by the choice of the variational mean field state (or equivalently the preprojected wavefunction) and that local Gutzwiller projection may not account for all of the important correlations.

The Gutzwiller variational approach has been applied to a variety of SU(2) quantum antiferromagnets; see for instance Refs. [35, 36, 37, 38, 39, 40, 41, 42, 43]. Many of these studies support the possibility of 2D spin liquids with gapless spin excitations. One advantage of extending the Gutzwiller variational approximation to SU(N) quantum antiferromagnets is that the approximation becomes more accurate as N increases. Indeed, since the gauge theory approach and the variational approach reduce to the same (exact) mean field theory at $N = 1$, but suffer different criticisms at finite N , it is interesting to compare results from both approaches as N is decreased systematically from $N = 1$ down to $N = 2$. The existence of some exact results for SU(N) quantum antiferromagnets in one and higher spatial dimensions [10] provides valuable checks not available in the SU(2) case. So motivated, we numerically explore

in this paper Gutzwiller wavefunctions for SU(N) spin models in the self-conjugate representation with Heisenberg bilinear and biquadratic interactions. In section 2 we compare the variational approach in 1D with exact results and analytical 1=N calculations. Section 3 focuses on the 2D square lattice. Comparison is made with 1=N calculations and with Assaad's quantum Monte Carlo results. We summarize and discuss the implications of our results in section 4. For the reader interested in the main results, phase diagrams in the different sections provide a quick overview of our conclusions.

2. One Dimension

We begin with a study of SU(N) spin models in 1D. The existence of a reliable phase diagram for the SU(4) spin chain [10] provides a valuable check on the quality of the variational wavefunctions. We first define the model and then compare the phase diagram of the SU(4) chain as obtained with the variational wavefunctions to the known result. Then we examine various correlation functions calculated from the Gutzwiller projected SU(N) Fermi gas wavefunction and compare the exponents so obtained to exact analytical results for the critical point in the SU(N) spin chain.

2.1. Models

For $N = 2$, the usual Heisenberg model is the only nearest-neighbor Hamiltonian that is both SU(2) symmetric and translationally invariant. In 1D we may write it as:

$$H_2 = \sum_i S_i \cdot S_{i+1}; \quad (1)$$

where the trace $\text{Tr}[S_i \cdot S_{i+1}]$ is simply a rewriting of the vector form $H_2 = 2 \sum_i S_i^x S_{i+1}^x$ with standard spin operators $S_i = \frac{1}{2} \mathbf{f}_i^y \sim \mathbf{f}_i$ in terms of the matrix form of the spin operators. It is well-known that the model has no long range order, but rather exhibits algebraically decaying antiferromagnetic spin correlations up to a multiplicative logarithmic factor.

For $N = 4$, the most general translationally-invariant nearest-neighbor Hamiltonian can have an additional biquadratic spin-spin interaction term:

$$H_4 = \cos \sum_i S_i \cdot S_{i+1} + \frac{\sin}{4} \sum_i [S_i \cdot S_{i+1}]^2; \quad (2)$$

where \cos parametrizes the relative strength of the Heisenberg and biquadratic terms. Whereas the usual bilinear Heisenberg interaction exchanges two fermions on adjacent sites, the biquadratic term exchanges two pairs of fermions. The antiferromagnetic region of the phase diagram of H_4 is generically gapped [17, 10, 44]. The Lieb-Schultz-Mattis theorem then says that these gapped phases must break translational symmetry in one way or another [45]. Tuning \cos leads to a variety of phases and phase transitions. For instance, positive \cos frustrates dimerization, and when \cos becomes sufficiently large, the dimerized phase is eliminated.

2.2. Phase Diagram of the SU(4) Model

The phase diagram of the SU(4) model, equation 2, was obtained in reference [10] and is shown in the inset to figure 1. It displays four phases: A fully polarized ferromagnet (FM), a dimerized phase (D), a phase with broken charge-conjugation symmetry (C), and, finally, a phase with broken translational symmetry and a 6-site unit cell (6-fold). The D to FM transition and the 6-fold to FM transition are both first order, while the D to C and the C to 6-fold state transitions are both continuous. We now describe these phases more precisely and present the results of calculations based upon the corresponding variational wavefunctions.

FM, Ferromagnet: The ground state of a fully polarized ferromagnet breaks the global SU(4) spin symmetry but no lattice symmetries. A simple and exact ground state wavefunction may then be constructed by placing any two of the four fermion flavors on the lattice, each site having the same two flavors. All other ground states can be obtained by global SU(4) rotations of the state. Because the Pauli exclusion principle prevents any fermion hopping in the FM state, it is straightforward to show that $\langle S(i)S(i+1) \rangle = \langle S(i)S(i+1) \rangle^2 = 1$, so that the exact ground state energy per site is

$$e_{FM}^{exact} = \cos \theta + \frac{1}{4} \sin \theta : \quad (3)$$

D, Dimerized: The dimerized phase is a spin gapped phase with a two fold ground state and a nonzero order parameter $\rho_D = \langle S(i)S(i+1) \rangle - \langle S(i-1)S(i) \rangle$ that takes on equal positive/negative values in the two ground states and is zero in a state with no broken symmetries. This phase does not break the SU(4) spin symmetry, but does break lattice translations (the ground state is invariant only under translation by two lattice spacings), and inversion symmetry about a lattice site. In order to obtain a wavefunction for this phase, we consider a mean field fermion Hamiltonian with alternating hopping strengths $(1 + \alpha)$ and $(1 - \alpha)$ on successive bonds:

$$H_D^0 = \sum_{i,j=1::4} (1 + (-1)^i) f_i^\dagger f_{i+1} + h.c. : \quad (4)$$

This starting Hamiltonian has the following favorable features: it is SU(4) symmetric, has a gap to fermion excitations (and thus a gap to spin excitations in mean field theory), and breaks the same lattice symmetries as the dimerized phase. In addition, the ground state of the Hamiltonian satisfies $\langle S(i) \rangle_0 = 0$ since it is particle-hole symmetric. The ground state of this mean field model is simply a product of four Slater determinants, one for each flavor of fermion, with the lowest half of the single particle states filled. Gutzwiller projecting the mean-field ground state leads to a variational ansatz for the dimerized phase of the spin model, with α being the variational parameter that we optimize by minimizing $\langle H_D \rangle$ to find the best variational ground state. We find that the dimerization strength, defined in the mean field problem via the variational parameter α , is nonzero at $\alpha = 0$ indicating that the SU(4) Heisenberg model has a dimerized ground state. With increasing α , the optimal α decreases and vanishes around $\alpha_c \approx 0.41(3)$, in reasonably good agreement with the exact result $\alpha_c = \tan^{-1}(1/2) \approx 0.4636$. We also

and that η increases in magnitude for negative β and approaches unity at large negative β , indicating that dimerization is nearly complete.

C, Charge-conjugation symmetry broken: The model H_4 is invariant under the global particle-hole transformation $f_i \rightarrow f_i^y$ and thus possesses charge-conjugation (C) invariance. In terms of the spin operators, the transformation takes the form $S^z(i) \rightarrow -S^z(i)$.

$S^z(i)$. The C phase corresponds to a phase in which this symmetry is spontaneously broken. This phase does not break the SU(4) spin symmetry but does break lattice symmetries as the ground states are invariant only under translation by two sites, and they break inversion symmetry about the bond centers. It is characterized by an order parameter made up of a triple product of spins: $\text{Tr}(S_i S_{i+1} S_{i+2})$. An extreme caricature of the state (analogous to the product state of nearest neighbor dimers) is an extended valence bond solid of site-centered SU(4) singlets formed from two flavors of fermions at a central site combined with a fermion from each of the two flanking sites. This product state is an exact ground state of model H_4 at the special point $\beta = \beta_c = \tan^{-1}(2/3)$.

The mean field Hamiltonian we use to obtain the preprojected wavefunction for the C-breaking state is

$$H_C^0 = \sum_{i,j=1::4}^X \sum_{h=1::4}^h f_i^y f_{i+1,j} + h.c. + t \sum_{i,j=1::4}^X (1)^i f_i^y f_{i+2,j} + h.c. : (5)$$

Nonzero t breaks the global particle-hole symmetry since it connects sites belonging to the same sublattice. The alternating sign of t on the odd and even sublattices breaks inversion symmetry about bond centers of the lattice, and generates a gap in the mean field fermion spectrum (and thus a gap to spin excitations in the mean field theory). Finally, the Hamiltonian is invariant under a global particle hole transformation followed by translation by one lattice spacing, and hence satisfies $hS^z(i) + S^z(i+1)i_0 = 0$. We can further modify the wavefunction to include a staggered chemical potential in order to obtain $hS^z(i)i_0 = 0$ at each site. However since the mean field state is projected into the correct Hilbert space that satisfies $S^z(i) = 0$ exactly, we choose to work with the simpler mean field Hamiltonian without this staggered chemical potential (we have checked that including the staggered chemical potential does not affect the results in any significant quantitative manner).

A check on the quality of this variational wavefunction for the C phase is provided by a comparison between the variational and exact ground state energy per site at the point $\beta = \tan^{-1}(2/3)$ where a C product is the exact ground state while the variational ground state exhibits nonzero t . The variational ground state energy at this point, $E_{\text{var}}(\beta) = 0.6934(10)$, is close to the exact result $E_{\text{exact}}(\beta) = \frac{\pi^5}{2^{13}} \approx 0.69337 \dots$.

Turning to general β , we find that the variational parameter t is zero for $\beta < 0.42(2)$, and increases monotonically for $\beta > 0.42(2)$. The β at which t first becomes nonzero thus seems to coincide (within numerical error) with the point where the dimerization parameter η vanishes ($\beta = 0.41(3)$).

6-fold degenerate state: The phase diagram of the SU(4) spin chain has two special points with enlarged SU(6) symmetry, and a gapped 6-fold degenerate phase is associated with one of these points[10]. We may understand the origin of the 6-

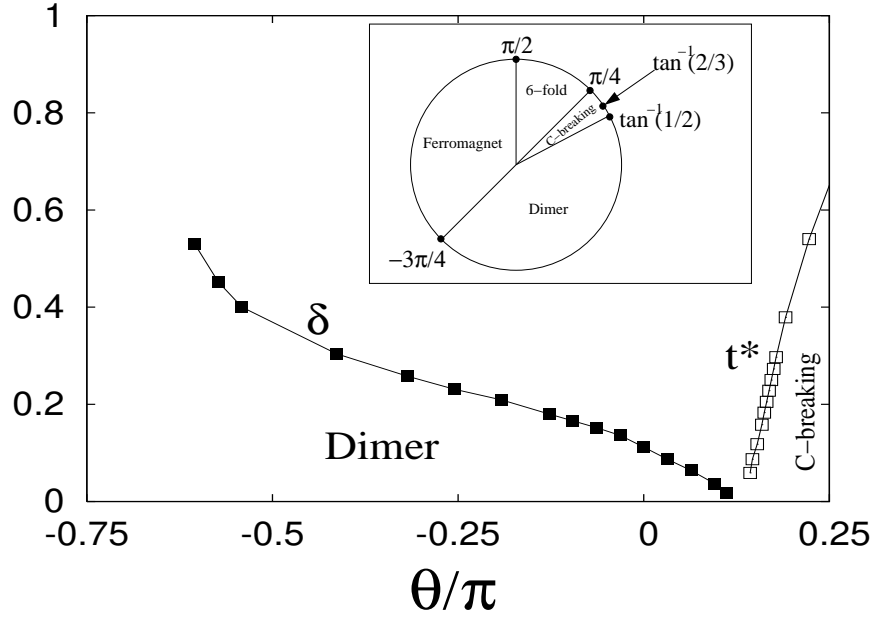


Figure 1. Variational calculation of the ground state energies of dimerized (D) and charge-conjugation broken (C) phases of the model Hamiltonian H_4 in equation 2. Both broken symmetries apparently vanish around $\theta = 0.42(3)$, hinting at a possible continuous phase transition with a gapless critical point that is reasonably well-described by the Gutzwiller projected 4-flavor Fermi gas wavefunction (see text). *Inset:* The full phase diagram, including the ferromagnetic and 6-fold symmetry broken phases, of the SU(4) spin chain with biquadratic interactions. The exact location of the D-C transition is at $\theta = \tan^{-1}(1/2) = 0.4636$. The point at which the C extended valence bond product state is an exact ground state is $\theta = \tan^{-1}(2/3)$.

fold degeneracy as follows: View the 6 possible states of the self-conjugate SU(4) representation (two distinct flavors chosen out of four possible ones) on each site as the six states of the fundamental representation of SU(6). Six such states, taken from six adjacent sites, can be combined into a SU(6) singlet. The resulting spin-gapped ground state breaks translational symmetry with a 6-site periodicity. Unfortunately we have not yet found a way to express the state in terms of the Slater determinants of single-particle wavefunctions, a proper description likely needs some form of pairing to capture the above physics. We therefore do not focus on this phase at present, postponing it to future study.

D-FM transition We know from the phase diagram of reference [10] that there is a first order D to FM transition. Since the dimerization order parameter appears to increase monotonically at larger negative values of θ , we may estimate the approximate location of the D-FM transition by comparing the energy of the FM state with a fully dimerized state ($\delta = 1$) that is just a product of nearest neighbor singlets on alternate bonds. The energy of this variational state can be found knowing that for neighboring uncorrelated sites (not on the same singlet bond) $\langle S(i)S(i+1) \rangle = 0$ and $\langle S(i)S(i+1) \rangle^2 = 5/3$, while for neighboring spins that form the singlet bond

hS(i)S(i+1)i = 5 and hS(i)S(i+1))²i = 25. This leads to

$$e_D^{-1} = \frac{5}{2} \cos + \frac{10}{3} \sin : \quad (6)$$

Comparing this energy with e_{FM}^{exact} , we find the variational estimate of the angle at which the dimer state becomes unstable to ferromagnetism to be $\frac{var}{D, FM} = \tan^{-1}(84=74)$

0.73, very close to the exact result $\frac{exact}{D, FM} = 3=4$. The error in the variational estimate of the transition angle is consistent with the fact that while the energy of the ferromagnet is obtained exactly, the energy of the dimer product state with e_D^{-1} is only an upper bound to the true ground state energy of the dimerized state at the transition. C-D transition The numerical coincidence of the values of θ at which θ and t vanish indicates that the transition between the D and C phases could be continuous even within the variational approach as in the rigorous phase diagram. We have not studied wavefunctions with coexisting t and θ broken symmetry parameters and cannot rule out the possibility that such a variational ansatz may have lower energy in the region close to the transition. We also cannot rule out the possibility that the variational approach leaves a very small window where $t = \theta = 0$ giving rise to a gapless phase. Assuming however that neither of these possibilities is realized, and that the transition between the two phases is continuous even within the variational approach, the projected half-filled Fermi gas state (with $\theta = t = 0$ in the mean field Hamiltonian) is a good candidate for the critical point describing the C-D transition. We turn next to a study of correlation functions of this wavefunction.

2.3. Correlation Functions for the Projected Fermi Gas at Various N

As the phase diagrams of the SU(2) and SU(4) spin chains are known [10], these provide good test cases for the method. At the critical point in the SU(N) chain, the exponents of the spin-spin and dimer-dimer correlation functions follow directly from equations (4.10) and (4.12) of reference [10], once the scaling dimension of the level $k = 1$ Wess-Zumino-Witten (WZW) field g is known. (The contribution of the currents J_L and J_R in equation (4.10) to the spin-spin correlation function is subleading, as the currents have dimension 1, greater than that of the g -field.) Reference [46] gives the dimension of a tower of WZW operators labeled by the integer a :

$$\begin{aligned} \dim(g) &= h + h \\ h &= h = \frac{a(N-a)}{2N}; \quad a = 1; 2; \dots; N; \end{aligned} \quad (7)$$

with $a = 1$ corresponding to the operator with smallest nontrivial dimension. The conformal charge $c = N - 1$ is correct as it equals the number of fermions in the corresponding SU(N) Hubbard model minus 1 due to the freezing out of charge fluctuations, leaving only $N - 1$ spin excitations. Now the exponent of the staggered part of the spin-spin correlation function, as well as the dimer-dimer correlation function, is twice the dimension of g , yielding $2 - 2/N$. This exponent reduces to the free fermion

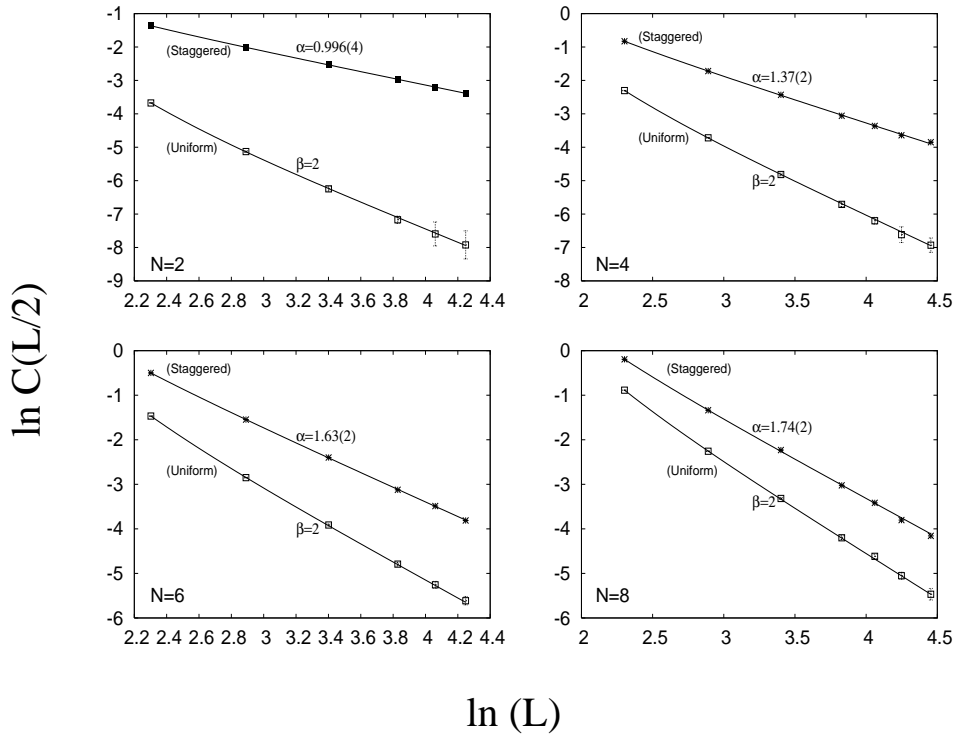


Figure 2. Logarithm of the staggered and uniform components of the spin-spin correlation function at distance $L=2$ plotted versus $\ln(L)$, for the projected free Fermi gas with N flavors (L denotes the number of sites of the spin chain). The uniform spin correlations appear to decay as $1/r^2$ for all N . The staggered spin correlations are enhanced at smaller N , and decay with the indicated exponents (see text for details).

value of 2 in the $N \rightarrow 1$ limit, and to 1 in the usual SU(2) Heisenberg chain, as it should.

How do correlation functions behave in the projected Fermi gas wavefunction for general N ? For $N = 2$ the Gutzwiller projected Fermi gas wavefunction at half-filling is the exact ground state of the Heisenberg model with $1/r^2$ interactions [47, 48]. It also correctly describes correlation functions of the ground state of the J1-J2 Heisenberg model at the critical point between the gapless spin liquid phase and the dimerized phase [49]. The spin-spin correlations of this wavefunction have been computed exactly [50, 51], but we are not aware of an exact result for its dimer-dimer correlations. We present numerical results for both correlations below. For $N = 4$, given the possibility that the projected free Fermi gas wavefunction at half-filling could be a candidate for the CD transition, we study spin-spin and dimer-dimer correlation functions of the wavefunction and compare to exact results from the field theory for this transition. We also examine the correlation functions in the projected Fermi gas wavefunction for $N > 4$ as such wavefunctions may describe multicritical points in the phase diagram of generalized SU($N > 4$) spin models.

Spin-spin correlations: At $N = 1$, the long distance behavior of the spin correlation function $C_{ss}(x) = \langle S(0)S(x) \rangle$ is given by mean field theory, $C_{ss}(x) \sim (1/x^2 +$

$(-1)^x = x^2$). In the opposite limit, $N = 2$, the spin correlations of the projected Fermi gas wavefunction have been calculated exactly by Gebhard and Vollhardt [50, 51] to be $C_{ss}(x) = (-1)^x \frac{3\text{Si}(x)}{2x}$, where $\text{Si}(x)$ is the sine integral function $\text{Si}(x) = \int_0^x dy \sin(xy) = y$. The long distance decay of the correlator is $C_{ss}(x) \sim \frac{(-1)^x}{x} \sim \frac{2}{x^2}$. Thus the staggered spin correlations decay more slowly for $N = 2$ than they do in mean field theory, while the uniform component continues to decay as $1/x^2$.

Incorporating gauge fluctuations perturbatively [20, 21] modifies the long distance spin correlations to:

$$C_{ss}(x) = \frac{A(-1)^x}{x^s} - \frac{B}{x^s} : \quad (8)$$

The $O(1/N)$ result for the exponents are $s_s = 2$ and $s_u = 2 - 2/N$; rather surprisingly, the latter exponent agrees with the exact result. Thus, gauge fluctuations enhance the staggered spin correlations over the mean field result, while the uniform component decays at the same rate $1/x^2$ as the mean field result.

In order to extract the exponent $s_s(N)$ from the numerical calculations on the Gutzwiller projected wavefunction for general N , we assume that the correlations are of the form

$$C_{ss}(x) = \frac{A_s(-1)^x}{x^{s_s}} - \frac{B_s}{x^2} : \quad (9)$$

In order to carry out finite size scaling, we consider the function

$$C(L=2) = (-1)^{L=2} C_{ss}(L=2) = \frac{A_s}{(L=2)^{s_s}} - \frac{B_s(-1)^{L=2}}{(L=2)^2} : \quad (10)$$

From this equation we can obtain the staggered and uniform components of the spin correlations via

$$C_{\text{stag}}(L) = \frac{1}{2} [C(L=2) + \frac{1}{2} (C(L=2+1) + C(L=2-1))] \quad (11)$$

$$C_{\text{unif}}(L) = \frac{1}{2} [C(L=2) - \frac{1}{2} (C(L=2+1) + C(L=2-1))] : \quad (12)$$

To leading orders in $1/L$, these functions take the form

$$C_{\text{stag}}^t(L) = \frac{A_s}{(L=2)^{s_s}} + \frac{A_{s-s}(1 + \frac{s_s}{L})}{(L=2)^{2+s_s}} + \frac{u_s}{(L=2)^4} \quad (13)$$

$$C_{\text{unif}}^t(L) = \frac{B_s}{(L=2)^2} - \frac{A_{s-s}(1 + \frac{s_s}{L})}{L^2 (L=2)^{s_s}} + \frac{v_s}{(L=2)^4} \quad (14)$$

We also obtain the staggered and uniform components of the spin correlation function data for various L using equation 12. We first fit the staggered correlations using the parameters $A_s; u_s; s_s$. Next we use this value of s_s and the parameters $B_s; v_s$ to fit to the uniform component of the spin correlations. The fits are shown in figure 2 for both the uniform and staggered components for cases $N = 2, 4, 6$, and 8 . This leads to the following estimates for various N : $s_s(2) = 0.996(4)$, $s_s(4) = 1.37(2)$, $s_s(6) = 1.63(2)$, and $s_s(8) = 1.74(2)$. These values are in remarkably good agreement with the exact value of the spin-spin correlation function exponent at the critical points of these chains, which for $N = 4$ lies at the continuous CD transition. We also find that the fitted

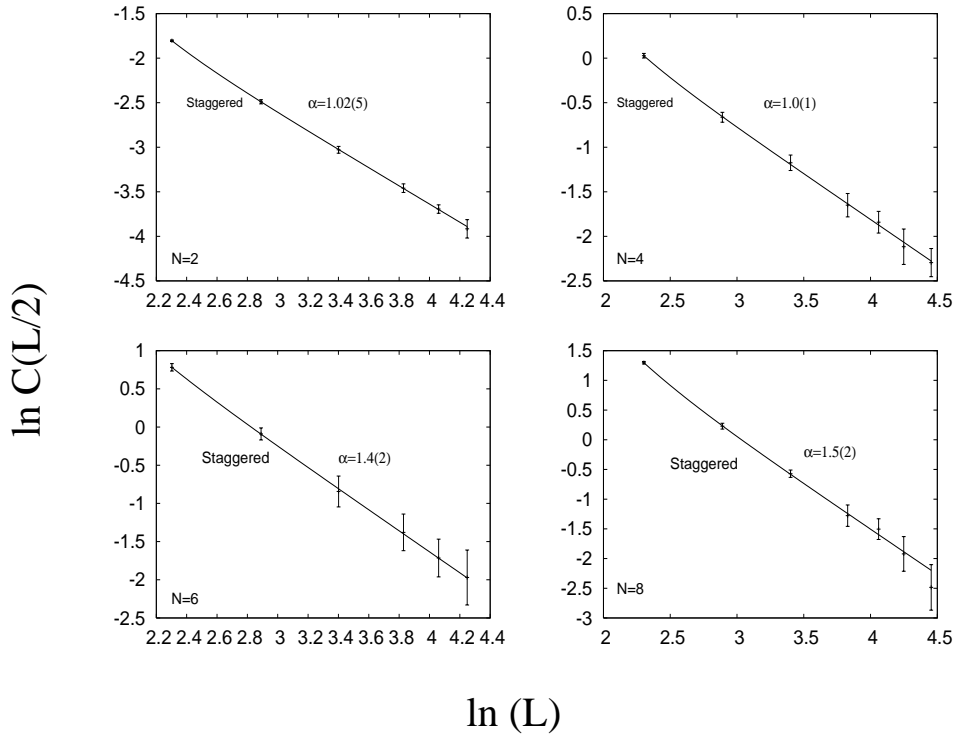


Figure 3. Logarithm of the alternating component of the dimer-dimer correlation function at distance $L=2$ plotted versus $\ln(L)$, for the projected free Fermi gas with N - flavors (L denotes the number of sites of the spin chain). The decay exponents are indicated (see text). The decay of the uniform correlation is much faster and the corresponding exponents have not been obtained reliably.

value of the amplitude ratio $A_s=B_s$ tends to unity as $N \rightarrow 1$, consistent with mean field theory. At present, we are unable to determine if the small differences between the exact results and the wavefunction calculations of $\chi_s(4)$ and $\chi_s(6)$ are real or an artifact of working with chains of less than 100 sites.

Dimer-dimer correlations: We have similarly evaluated the dimer-dimer correlations in the projected N - flavor Fermi gas in 1D, namely $C_{dd}(x) = \langle S(0)S(1)S(x)S(x+1) \rangle$. The finite size scaling of this correlation function is analyzed in a manner similar to that of the spin-spin correlation function, except for one significant difference. We fit to $C_{dd}(x) = A_d(1)^x x^{-\alpha_d}$, dropping the uniform component that decays much more rapidly, so that we cannot extract its behavior reliably compared to the staggered component. The finite size scaling plots of the correlation function are shown in Figure 3, along with estimates of α_d for various N . We find $\alpha_d(2) = 1.02(5)$, $\alpha_d(4) = 1.0(1)$, $\alpha_d(6) = 1.4(2)$, and $\alpha_d(8) = 1.5(2)$. The projected Fermi gas wavefunction thus has strongly enhanced alternating dimer correlations in addition to enhanced staggered spin correlations. For $N = 2$, it is in agreement with the exact result $\alpha_d = 2 - 2/N$. For $N > 2$, the variational wavefunction exponents $\alpha_d(N) < \alpha_s(N)$ (most significantly for $N = 4$) while exact results suggest $\alpha_s(N) = \alpha_d(N) = 2 - 2/N$. Thus, the projected Fermi gas wavefunction does not quite capture this aspect of the C-D critical point at

$N = 4$, although it does capture the existence of strongly enhanced staggered spin and alternating dimer correlations, decaying in power-law fashion with anomalous exponents. Having shown that the variational wavefunctions provide a reasonably good description of SU(N) spin models in 1D, we next turn to 2D examples.

3. Two Dimensional Square Lattice

Buoyed by the successful description of the SU(N) spin chains with variational wavefunctions, we now apply the same methodology to the study of 2D SU(N) spin models. Much less is known reliably about the phase diagrams of such models at finite N . An interesting gapless spin liquid discovered some time ago in the large- N limit of the self-conjugate SU(N) Heisenberg model with biquadratic interactions to thwart dimerization is the π -flux state [16, 17]. At $N = 1$, where projection to exactly $N=2$ fermions per site does nothing to the mean field state, the π -flux state corresponds to the ground state of fermions (at half-filling) hopping on the square lattice while sensing a (spontaneously generated) fictitious magnetic flux of π per elementary plaquette [16]. It supports gapless linearly dispersing Dirac fermion excitations about two nodes in the reduced Brillouin zone. Spin-1 excitations, which are bilinears of the Dirac fermions, are therefore gapless at the wavevectors spanning the Dirac nodes: $(\pi/2; \pi/2)$, $(\pi/2; 0)$, $(0; \pi/2)$, and $(0; 0)$. For the case of the ordinary nearest-neighbor SU(2) Heisenberg antiferromagnet on the square lattice, Gutzwiller projecting this mean field wavefunction leads to a variational ground state with power law decay of staggered spin correlations (as there is no long range magnetic order) and an energy $(1/2)\hbar S \langle \mathbf{S}_i \mathbf{S}_{i+\hat{x}} \rangle = 0.319$ per bond. The true ground state of the Heisenberg model is known to be Neel ordered, with a spin moment of about 60% of the classical value, and $(1/2)\hbar S \langle \mathbf{S}_i \mathbf{S}_{i+\hat{x}} \rangle = 0.3346$ per bond. Since the π -flux state is close to the true ground state, both energetically and in its display of (quasi) long-range antiferromagnetic correlations, we focus on the part of the phase diagram of the SU(N) Heisenberg model (with possible additional biquadratic interactions) that is close to that of the π -flux phase. More precisely, we investigate instabilities of the π -flux state towards various translational- and SU(N)-symmetry breaking orders. This point of view was advocated in earlier studies of the $N = 2$ case [37, 18], and in more recent work by Ghaemi and Senthil [32].

We begin with the SU(N) Heisenberg model in the absence of biquadratic interactions, and compare the resulting variational phase diagram with that from a recent quantum Monte Carlo (QMC) study of the same model [34]. We then turn to the nature of the spin and dimer correlations of the SU(4) projected π -flux state and compare the correlation functions to results from recent analytical large- N studies [29] and QMC calculations [34]. Finally, we examine the variational phase diagram of the SU(4) and SU(6) models with a biquadratic interaction added to thwart instabilities. For $N = 6$, we find a (small) window of parameters where the projected π -flux state appears to be stable towards Neel, spin Peierls and broken-C ordering. Our work thus hints at the existence of a stable SU(6) gapless spin liquid phase in a simple

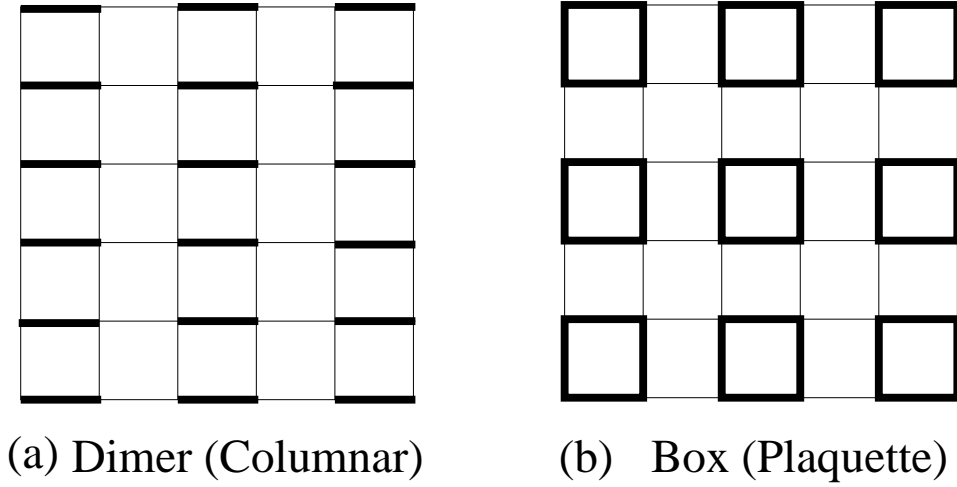


Figure 4. The two candidate spin Peierls ground states of the 2D SU(N) spin models explored in this paper. The thick lines indicate bonds with a larger singlet expectation value $\langle \mathbf{S}_i \cdot \mathbf{S}_j \rangle_{ij}$.

two dimensional microscopic spin model.

3.1. Phase Diagram of the SU(N) Heisenberg model

The Hamiltonian of the 2D antiferromagnetic SU(N) Heisenberg model is

$$H_{2D} = \sum_{\langle i,j \rangle} \mathbf{S}_i \cdot \mathbf{S}_j; \quad (15)$$

where $\langle i,j \rangle$ denotes nearest neighbor sites on the square lattice. As discussed above, the projected π -ux wavefunction with $N=2$ fermions at each site is an attractive starting point to describe the ground state of the model. The mean field ansatz for the π -ux phase is

$$H_{\pi\text{-ux}} = \sum_{\langle i,j \rangle} t_{ij} e^{ia_{ij}} f_i^y f_j + \text{h.c.}; \quad (16)$$

with $t_{ij} = t$ and a gauge choice of $a_{i,i+\hat{x}} = \frac{\pi}{4} (1)^{x_i+y_i}$ and $a_{i,i+\hat{y}} = \frac{\pi}{4} (1)^{x_i+y_i}$. Here we examine the instability of the variational state obtained by Gutzwiller projecting the ground state of this mean field Hamiltonian towards Neel and spin Peierls ordering. (We have also checked that there are no instabilities to time-reversal symmetry broken states or states with broken charge-conjugation symmetry. These wavefunctions have higher energy, so the ground states exhibit only Neel or spin Peierls order.)

To account for the possibility of Neel ordering we modify the mean-field Hamiltonian with the addition of a SU(N) symmetry breaking perturbation that favors two-sublattice ordering, with any chosen set of $N=2$ flavors favored on one sublattice, and the remaining $N=2$ flavors on the other sublattice:

$$H_{\text{neel}} = H_{\pi\text{-ux}} + h_N \sum_{i; N=2} (1)^{x_i+y_i} f_i^y f_i + h_N \sum_{i; >N=2} (1)^{x_i+y_i} f_i^y f_i; \quad (17)$$

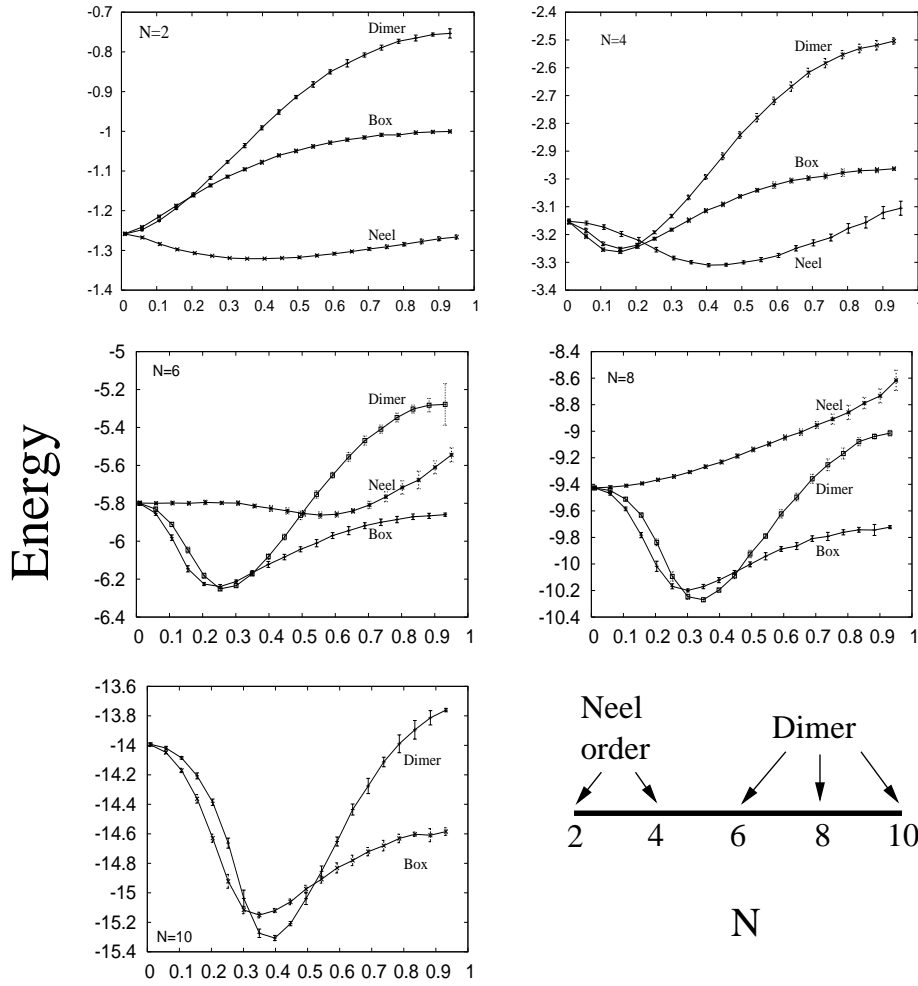


Figure 5. Energy minimization plots for even $N = 2$ to 10 . The x-axis is the variational parameter appropriate to the broken symmetry being studied. The y-axis is the (dimensionless) energy ($\hbar^{-1} E$) for the model of equation 15). We conclude that the SU(N) Heisenberg model exhibits Neel order for $N = 2$ and 4 , and spin Peierls ordering of the columnar dimer type for $N > 4$.

In order to study spin Peierls ordering, we focus on two different types of broken symmetry states, "dimer order" (more precisely, columnar dimer order) and "box order" (also called plaquette order). In the dimer state, spins prefer to form singlets on nearest neighbor bonds, and the bonds organize as shown in figure 4 (a). Three other equivalent, but distinct, states are obtained by x translations and $\pi/2$ rotations of the displayed pattern. The mean field ansatz for the preprojected wavefunction of the dimer state is obtained by modulating t_{ij} such that $t_{i,ji+\hat{x}} = 1 + \delta_D (-1)^{x_i}$ and $t_{i,ji+\hat{y}} = 1$. The box state has a different broken symmetry; the strength of singlet bonds is shown in figure 4 (b). Three other equivalent box states are obtained by x and y translations of the displayed pattern. For the box state, we modulate t_{ij} such that $t_{i,ji+\hat{x}} = 1 + \delta_B (-1)^{x_i}$ and $t_{i,ji+\hat{y}} = 1 + \delta_B (-1)^{y_i}$.

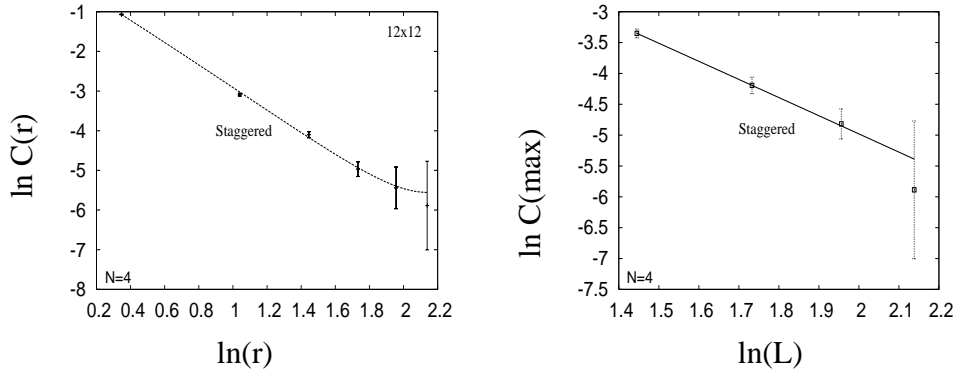


Figure 6. Spin-spin correlation function of the 2D projected π -flux wavefunction for $N = 4$ and a system with L^2 sites. The label $C(\max)$ denotes the correlation function evaluated for points with the maximum separation, $L = \sqrt{2}$, on the $L \times L$ square lattice.

The mean field box and dimer states have a single particle gap to fermionic excitations and thus also a spin gap. These spin Peierls ordered states as well as the Neel state are invariant under a particle-hole transformation (followed by a global $SU(4)$ spin rotation in the case of the Neel state), and thus are at half-filling. We project these mean field ansatz to obtain variational spin wavefunctions for the Heisenberg model. The phases of the $SU(N)$ Heisenberg model are then obtained by looking for the state with the lowest variational energy. As summarized in figure 5, we find that the Neel ordered state has the lowest energy for $N = 2$ and 4, while the dimer state (i.e., columnar dimer) state has the lowest energy for $N > 4$. For $N = 2$, this result is in agreement with other numerical work [52, 53, 34]. The presence of spin Peierls order for large values of N is in agreement with $1/N$ calculations [16]. The same pattern of (columnar) dimer order was also predicted for various representations of $SU(N)$ antiferromagnets in large- N calculations by Read and Sachdev [54, 55]; these predictions have received some numerical support [56], with Neel order reported for $N \leq 4$ and dimer order for $N > 4$, identical to the phase diagram in figure 5.

3.2. Correlation Functions of the Projected $SU(4)$ π -Flux State

To make contact with a recent QMC study of the $SU(4)$ Heisenberg model [34], we turn now to the spin-spin and dimer-dimer correlations of the projected π -flux wavefunction. The analysis of these correlations is done in a manner similar to that in 1D, except that we focus only on the strong nonzero-wavevector component (near (π, π) for the spin order and near $(\pi, 0)$ for the dimer correlations) and ignore the uniform components. The uniform component of the spin-spin correlation in 2D is expected to decay quickly, as $1/r^4$, and is therefore numerically harder to evaluate.

The results for the finite size scaling of the staggered spin-spin correlation function are shown in figure 6, together with the correlation function results for the 12×12 system. We find that the staggered spin-spin correlation function decays as $1/r$ with

$\alpha_s(4) = 3.0(4)$. This value is in excellent agreement with large- N calculations [29, 21] that find $\alpha_s(N) = 4/128 = (3/2N)$. However, the exponent $\alpha_s(4)$ is much larger than that found in a QMC simulation by Assaad [34]. Although the QMC calculation suggested a spin liquid ground state of the ν -ux type for the SU(4) Heisenberg model, Assaad found $\alpha_s = 1.12$. The origin of the large difference needs further exploration, and we speculate on a possible reason for the discrepancy in the final section.

A numerical analysis of the dimer-dimer correlation function at $Q = (\pi; 0)$ for the $N = 4$ projected ν -ux wavefunction yields $\alpha_d(4) = 2.1(8)$; the larger error on the dimer-dimer correlation function exponent stems from having fewer Monte Carlo samplings of the wavefunction since the dimer-dimer correlation function takes more time to evaluate. We conclude that Gutzwiller projection strongly enhances both the spin-spin and the dimer-dimer correlations relative to the mean field result. In this sense, the projected ν -ux state is indeed the "mother of many competing orders" [29]! However, we have not confirmed yet that the projected ν -ux wavefunction is an algebraic spin liquid phase with enlarged SU(2N) symmetry leading to $\alpha_d = \alpha_s$ [29]. We are currently carrying out further numerical calculations to reduce the error bars on the exponents and to better test this prediction quantitatively.

3.3. Adding Biquadratic Interactions for $N = 4$ and $N = 6$

The inclusion of the biquadratic interaction lead to a rich phase diagram in the case of the SU(4) spin chain. Motivated by this physics, we pursue here a variational study of the 2D square lattice model with Heisenberg bilinear and biquadratic interactions for SU(4) and SU(6). As in 1D, the 2D model is defined by the nearest-neighbor Hamiltonian:

$$H_4 = \cos \sum_{\langle i,j \rangle} \mathbf{S}(i) \cdot \mathbf{S}(j) + \frac{\sin}{4} \sum_{\langle i,j \rangle} [\mathbf{S}(i) \cdot \mathbf{S}(j)]^2; \quad (18)$$

where $\langle i,j \rangle$ refer to nearest neighbor sites on the 2D square lattice. Exact diagonalization and the density matrix renormalization group are inadequate tools to study the phase diagram of the two dimensional model. For spin Hamiltonians without a sign problem, QMC has proved to be the most reliable numerical tool in 2D, but the case of a positive biquadratic spin interaction cannot be studied reliably because it is a frustrating interaction that introduces the sign problem. Given the success of the variational approach in 1D we have reason to hope that the method may also provide a good guide to two dimensions, although we explore only a limited class of variational states. We consider the fully polarized ferromagnet FM, the (columnar) dimer state D, the Neel antiferromagnet N, the broken charge-conjugation symmetry state C, and the projected ν -ux state.

FM, Ferromagnet: The ground state of a fully polarized ferromagnet in 2D breaks global SU(N) spin symmetry but no lattice symmetries. An exact ground state wavefunction may be constructed by placing any two of the four fermion flavors on each lattice site, each site having the same two flavors. All other ground states can be

obtained by global SU(N) rotations of this state. Exactly as in 1D, because the Pauli exclusion principle prevents any fermion hopping in the FM state, it is straightforward to show that $\langle S(i)S(i+1) \rangle = N/4$ and $\langle S(i)S(i+1) \rangle^2 = N^2/16$, so that the exact ground state energy per site is

$$e_{\text{FM}}^{\text{exact}}(N) = \frac{N}{2} \cos \theta + \frac{N^2}{32} \sin^2 \theta : \quad (19)$$

D, Dimer: The columnar dimer state appeared in the phase diagram of the pure bilinear Heisenberg model and hence was discussed above in subsection 3.1. The only difference here is that we minimize the energy with respect to θ_D at each value of θ . The energy of the perfectly dimerized state for $N = 4, 6$ is

$$e_D^{\text{var}}(\theta_D = 1; N = 4) = \frac{5}{2} \cos \theta + \frac{15}{4} \sin^2 \theta \quad (20)$$

$$e_D^{\text{var}}(\theta_D = 1; N = 6) = \frac{21}{4} \cos \theta + \frac{1197}{80} \sin^2 \theta : \quad (21)$$

N, Neel: The Neel state with long range antiferromagnetic order was also discussed above. Here we minimize the energy with respect to the staggered magnetic field h_N at each θ . We emphasize that the classical antiferromagnetic state (obtained in the limit $h_N \rightarrow 1$) has a much higher energy than the optimal antiferromagnetic ground state at finite h_N in the relevant region of the phase diagram.

C, Charge-conjugation symmetry broken: The C phase is obtained by projecting the ground state of the mean field Hamiltonian

$$H_C^0 = H_{\text{ux}} + t \sum_{i,j=1 \dots 4} \sum_{\alpha} (1 - \gamma_i^{\alpha}) f_{i+2\alpha}^y + f_i^y f_{i+2\alpha}^y + h \sum_i \sigma_i^z ; \quad (22)$$

the 2D generalization of equation 5. The intra-sublattice hopping t gaps out the Dirac nodes of fermionic excitations in the $-ux$ state and thus leads to a spin gap in the mean field spectrum.

, The $-ux$ state: This gapless spin liquid state was also introduced earlier. This state does not have any variational parameters and is thus the most constrained state of the wavefunctions that we study. We leave for future work possible variational modifications of the state that preserve all lattice and spin symmetries. Since the $-ux$ state is a gapless state, it is important to study it under conditions such as particular system sizes that permit gapless nodes to appear at the mean field level. We find that the phase is artificially stabilized on lattices that do not permit the nodal wavevectors.

3.4. Phase diagram of the SU(4) spin model

We obtain the variational phase diagram shown in the left panel of figure 7 from an evaluation of the energy of the various SU(4) states. The ground state appears to generically exhibit broken symmetry. The D-FM, D-N and the C-FM transitions appear strongly first order due to level crossings. As in 1D, the ground state is nearly completely dimerized at the D-FM transition. The location of the D-FM transition is therefore simply and reliably estimated by studying a dimer

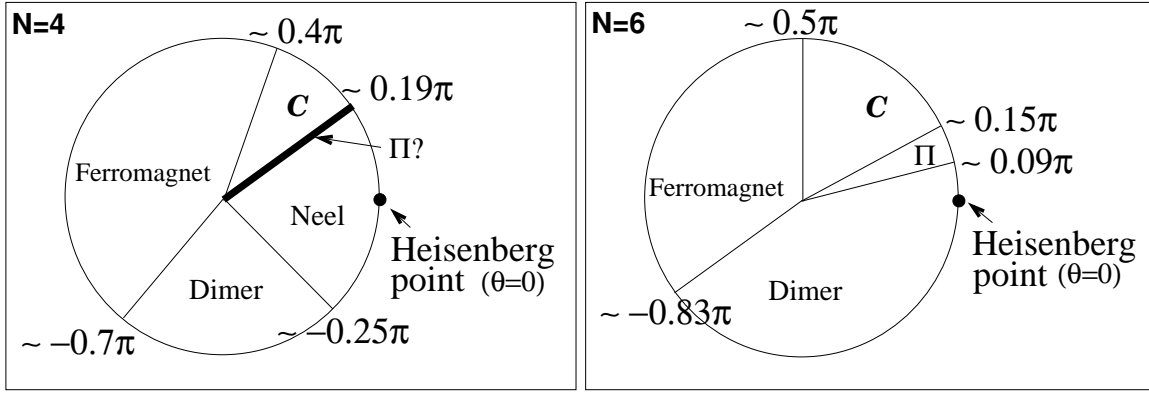


Figure 7. Phase diagram of the SU(4) and SU(6) spin models of equation 18, with Heisenberg bilinear and biquadratic interactions, on the 2D square lattice. Phases appearing here are the Neel phase, the ferromagnet, the columnar dimer phase, the broken charge-conjugation symmetry phase (C), and the π -ux spin-liquid phase (π). The thick line labeled π in the $N = 4$ phase diagram indicates that the projected π -ux state could either be stable over a thin sliver region ($0.18 < \beta = < 0.20$) or instead there may be a direct transition at $\beta = 0.19$ between the Neel and C phases. See text for details.

product wavefunction as the variational state for D. Setting $e_{FM}^{\text{exact}} = e_D^{\text{var}}(\beta_D = 1)$ leads to $\tan^{-1}(18/13) \approx 0.7$.

Due to limits on numerical accuracy and on system sizes (up to 10×10 for variational optimization), we are unable to determine whether there is a direct $N \rightarrow C$ transition at $\beta = 0.19$ or a thin sliver of the π -ux phase that intervenes between these two phases for $0.18 < \beta = < 0.20$. Since the Neel and C states are both deformations of the π -ux state, it is possible for a direct continuous transition to occur between them, with the projected π -ux state being a possible candidate for the critical point. However the addition of variational parameter(s) to improve short distance correlations of the projected π -ux state could in fact stabilize this state. We are examining this issue more carefully, and comment further on this point in the final section.

3.5. Phase diagram of the SU(6) spin model

The variational phase diagram is shown in the right panel of figure 7. Strikingly the Neel phase is completely replaced by the dimerized phase at $N = 6$, and the biquadratic interaction appears to stabilize the π -ux state over a small window of β . Of course within the variational approach one cannot rule out the possibility that π may be unstable to some other more complicated or exotic broken symmetries that have not been considered.

The D \rightarrow FM, D \rightarrow N and the C \rightarrow FM transitions appear strongly first order again due to level crossings. Since the ground state is nearly completely dimerized at the D \rightarrow FM transition the location of this transition is reliably estimated by studying a dimer product wavefunction as the variational state for D. Setting $e_{FM}^{\text{exact}} = e_D^{\text{var}}(\beta_D = 1)$

leads to $\tan^{-1}(\frac{\text{var}_{\text{FM}}}{660-1107}) = 0.83$.

4. Summary and Discussion

We have used Gutzwiller projected variational wavefunctions to deduce phase diagrams of SU(N) antiferromagnets with Heisenberg bilinear and biquadratic interactions in one and two spatial dimensions. In one dimension, the SU(4) variational phase diagram is in very good agreement with exact results. The spin and dimer correlations of the projected Fermi gas wavefunction with N fermion flavors are also in reasonably good agreement with $1/N$ calculations and exact results. Based on these results, the projected free fermion state with N fermion flavors appears to provide a good approximation of the critical points of SU(N) spin chains, and in particular it is a good description of the critical point between dimerized and broken charge-conjugation symmetry phases in the SU(4) model.

On the two dimensional square lattice the pure bilinear Heisenberg model exhibits Neel order for $N = 2$ and 4 and columnar dimer order for $N > 4$. Biquadratic interactions of positive sign appear to destabilize the Neel state, as the Neel order diminishes and gives way to a broken charge-conjugation symmetry phase via either a small sliver of the ν -ux spin liquid or by a continuous transition that is well described by the projected ν -ux state.

The spin and dimer correlations of the projected SU(4) ν -ux state are in reasonable agreement with analytical $1/N$ calculations. However the spin-spin correlations are quite different from those reported in QMC calculations by Assaad [34]. While that study finds a spin liquid ground state for the SU(4) Heisenberg model, apparently of the ν -ux type, the spin correlations decay much more slowly than those predicted on the basis of $1/N$ calculations or our variational calculation. Based on the variational study of model equation 18 with biquadratic interactions, we find that there could either be a thin sliver of the ν -ux phase or a direct continuous Neel-C transition at $\beta = 0.19$. In the exact phase diagram this transition point, or the sliver of the ν -ux phase, might occur even closer to the pure bilinear Heisenberg point. If this in fact is the case, a continuous Neel-C transition with a ν -ux state at the transition point (or a direct Neel- transition if a region of stable ν -ux spin liquid exists) could strongly influence the ground state of the pure SU(4) Heisenberg model as studied by QMC [34]. This hypothesis suggests that it may be numerically difficult to tell whether the correct ground state of the SU(4) Heisenberg model is a ν -ux spin liquid or a Neel ground state with a much reduced staggered magnetization. It could also account for the discrepancy in the spin correlations between the QMC on one hand and the $1/N$ and variational calculations on the other. Further studies of the SU(4) Heisenberg model with biquadratic interactions might shed light on this issue.

The SU(6) model does not appear to support a Neel phase at all. Instead biquadratic interactions open up a small window of ν -ux phase between the dimerized and broken charge-conjugation symmetry phases. We checked for instabilities of

the Ψ_{flux} state towards Neel order (characterized by non-zero $\langle S_i^z S_{i+j}^z \rangle$), dimer order (modulations in $\langle S_i^z S_{i+j}^z \rangle$) and C-breaking (modulations in $\langle S_i^z S_{i+j}^z S_{i+k}^z \rangle$) and found it to be stable against all three. However, we cannot rule out instabilities towards other more exotic broken symmetries characterized by more complicated order parameters. While the dimerized ground state at Heisenberg point also appears to be close to a spin liquid phase from our phase diagram, it is less likely to be influenced by proximity to such a critical point as the dimerized phase has a spin gap rendering it more stable to critical fluctuations than the Neel phase. This picture is consistent with Assaad's QMC results, with a dimerized ground state reported for the SU(6) Heisenberg model.

Finally, an exact C-breaking ground state of a 2D SU(8) spin model is known at a special point in parameter space [10] and it could be used as an additional test of the variational approach, which we have shown to be quite successful in describing a wide class of SU(N) antiferromagnets in one and two dimensions.

Acknowledgments

We thank F. Assaad, P. Fendley, M. Hemele, P. Lee, and T. Senthil for useful discussions and correspondence. This work was supported in part by the National Science Foundation under grant No. DMR-0213818 (JBM) and by the National Sciences and Engineering Research Council of Canada (AP). This work was initiated during the "Exotic Order and Criticality in Quantum Matter" program at the Kavli Institute for Theoretical Physics supported in part by the NSF under grant No. PHY 99-074. AP also thanks the Aspen Center for Physics Summer Program on "Gauge Theories in Condensed Matter Physics" where part of this work was completed.

References

- [1] Fazekas P and Anderson P W, "On the ground state properties of the anisotropic triangular antiferromagnet," 1974 *Phil. Mag.* 30, 423
- [2] For a review see: Misguich G and Lhuillier C, "Two-dimensional quantum antiferromagnets," in *Frustrated Spin Systems*, ed. H. T. Diep (World-Scientific 2005) (80 pages on cond-mat/0310405)
- [3] Coldea R, Tennant D A, Tsvetk A M, and Tyliczynski Z, "Experimental Realization of a 2D Fractional Quantum Spin Liquid," 2001 *Phys. Rev. Lett.* 86, 1335
- [4] Coldea R, Tennant D A, and Tyliczynski Z, "Extended scattering continua characteristic of spin fractionalization in the two-dimensional frustrated quantum magnet Cs_2CuCl_4 observed by neutron scattering," 2003 *Phys. Rev. B* 68, 134424
- [5] Shimizu Y, Miyagawa K, Kanoda K, Maesato M, and Saito G, "Spin liquid state in an organic Mott insulator with a triangular lattice," 2003 *Phys. Rev. Lett.* 91, 107001
- [6] Kurosaki Y, Shimizu Y, Miyagawa K, Kanoda K and Saito G, "Mott transition from spin liquid to Fermi liquid in the spin-frustrated organic conductor $-(\text{ET})_2\text{Cu}_2(\text{CN})_3$," 2005 *Phys. Rev. Lett.* 95, 177001.
- [7] Robert J, Simonet V, Canals B, Balbu R, Bordet P, Lejay P and Stunault A, "Spin-liquid correlations in the Nd-Langasite anisotropic kagome antiferromagnet" 2006 *Phys. Rev. Lett.* 96, 197205

- [8] Anderson P W, "The resonating valence bond state in La_2CuO_4 and superconductivity," 1987 Science 235, 1196
- [9] Baskaran G, Zou Z, Anderson P W, "The resonating valence bond state and high- T_c superconductivity { A mean field theory," 1987 Solid.State.Comm .63, 973
- [10] Aleck I, Arvas D P, Marston J B, and Rabson D A, "SU(2N) Quantum Antiferromagnets with Exact C-Breaking Ground States," 1991 Nucl.Phys.B 366, 467
- [11] Honerkamp C and Hofstadter W, "Ultracold fermions and the SU(N) Hubbard model," 2004 Phys. Rev. Lett. 92, 170403
- [12] Hofstadter Walter, "Flavor degeneracy and effects of disorder in ultracold atom systems," 2005 cond-mat/0504113 Adv. Solid State. Phys. (in press).
- [13] Buchler H P, Hermele M, Huber S D, Fisher Matthew P A, and Zoller P, "Atomic quantum simulator for lattice gauge theories and ring exchange models," 2005 Phys. Rev. Lett. 95, 040402
- [14] Onufriev A and Marston J B, "Enlarged Symmetry and Coherence in Arrays of Quantum Dots," 1999 Phys. Rev. B 59, 12573
- [15] Penc K, Mambri M, Fazekas P and Mila F, "Quantum phase transition in the SU(4) spin-orbital model on the triangular lattice," 2003 Phys. Rev. B 68, 012408 (2003), and references therein
- [16] Aleck I and Marston J B, "Large-N Limit of the Hubbard-Heisenberg Model: Implications for High- T_c Superconductors," 1988 Phys. Rev. B 37, 3774
- [17] Marston J B and Aleck I, "Large-N Limit of the Hubbard-Heisenberg Model," 1989 Phys. Rev. B 39, 11538
- [18] Marston J B, "Instantons and Massless Fermions in $2 + 1$ Dimensional QED and Antiferromagnets," 1990 Phys. Rev. Lett. 64, 1166
- [19] Marston J B, "Absence of Instanton Induced Spin-Peierls Order in the Flux Phase," 1990 Phys. Rev. B 42 (Rapid Comm.), 10804
- [20] Kim D on H and Lee Patrick, "Theory of spin excitations in undoped and underdoped cuprates," 1999 Annals of Physics 272, 130
- [21] Rantner Walter and Wen Xiao-Gang, "Spin correlations in the algebraic spin liquid: Implications for high T_c superconductors," 2002 Phys. Rev. B .66, 144501
- [22] Vafeck O, Tesanovic Z, Franz M, "Relativity Restored: Dirac Anisotropy in QED_3 ," 2002 Phys. Rev. Lett. 89, 157003
- [23] Franz M, Pereg-Barnea T, Sheehy D E, Tesanovic Z, "Gauge invariant response functions in Algebraic Fermi liquids," 2003 Phys. Rev. B 68, 024508
- [24] Herbut I F, Seradjeh B H, Sachdev S, and Murthy G, "Absence of U(1) spin liquids in two dimensions," 2003 Phys. Rev. B 68, 195110
- [25] Herbut I F and Seradjeh B H, "Permanent confinement in compact QED_3 with fermionic matter," 2003 Phys. Rev. Lett. 91, 171601
- [26] Kaveh K and Herbut I F, "Chiral symmetry breaking in QED_3 in the presence of irrelevant interactions: A renormalization group study," 2005 Phys. Rev. B 71, 184519
- [27] Hermele M, Senthil T, Fisher Matthew P A, Lee Patrick A, Nagaosa Naoto, and Wen Xiao-Gang, "Stability of U(1) spin liquids in two dimensions," 2004 Phys. Rev. B 70, 214437
- [28] Tanaka Akihiro and Hu Xiao, "Many-body spin Berry phases emerging from the flux state: Competition between antiferromagnetism and the valence-bond-solid state," 2005 Phys. Rev. Lett. 95, 036402
- [29] Hermele M, Senthil T, and Fisher Matthew P A, "Algebraic spin liquid as the mother of many competing orders," 2005 Phys. Rev. B 72, 104404
- [30] Nogueira Flavio S and Kleinert Hagen, "Quantum electrodynamics in $2 + 1$ dimensions, confinement, and the stability of U(1) spin liquids," 2005 Phys. Rev. Lett. 95, 176406
- [31] Lee Sung-Sik and Lee Patrick A, "U(1) gauge theory of the Hubbard model: Spin liquid states and possible application to $-(\text{BEDT-TTF})_2\text{Cu}_2(\text{CN})_3$," 2005 Phys. Rev. Lett. 95, 036403
- [32] Ghaemi Pouyan and Senthil T, "Neel order, quantum spin liquids and quantum criticality in two dimensions," 2006 Phys. Rev. B 73, 054415

- [33] Buchta K, Legeza O, Szirmai E and Solym J, "Mott transition and dimerization in the one-dimensional SU(N) Hubbard model," 2006 cond-mat/0607374
- [34] Assaad F F, "Phase diagram of the half-filled two-dimensional SU(N) Hubbard-Herbert model: A quantum Monte Carlo study," 2005 Phys. Rev. B 71, 075103
- [35] Zhang F C, Gros C, Rice T M, and Shiba H, "A renormalized Hamiltonian approach to a resonant valence bond wavefunction," 1988 Superconducting Science and Technology 1, 36
- [36] Gros C, "Physics of Projected Wavefunctions," 1989 Annals of Physics 189, 53
- [37] Hsu T C, "Spin waves in the flux-phase description of the $S = 1/2$ Heisenberg antiferromagnet," 1990 Phys. Rev. B 41, 11379
- [38] Paramakanti Arun, Randeria Mohit, and Trivedi Nandini, "Projected wave functions and high temperature superconductivity," 2001 Phys. Rev. Lett. 87, 217002
- [39] Paramakanti Arun, Randeria Mohit, and Trivedi Nandini, "High temperature superconductors: A variational theory of the superconducting state," 2004 Phys. Rev. B 70, 054504
- [40] Yunoki S and Sorella S, "Resonating valence bond wave function for the two dimensional fractional spin liquid," 2004 Phys. Rev. Lett. 92, 157003
- [41] Yunoki S and Sorella S, "Two spin liquid phases in the spatially anisotropic triangular Heisenberg model," 2006 Phys. Rev. B 74, 014408
- [42] Gan J Y, Chen Yan, Su Z B, and Zhang F C, "Gossamer superconductivity near antiferromagnetic Mott insulator in layered organic conductors," 2005 Phys. Rev. Lett. 94, 067005
- [43] Motrunich Olexei I, "Variational study of triangular lattice spin-1/2 model with ring exchanges and spin liquid state in $-(\text{ET})_2\text{Cu}_2(\text{CN})_3$," 2005 Phys. Rev. B 72, 045105
- [44] Szirmai E and Solym J, "Mott transition in the one-dimensional SU(N) Hubbard model," 2005 Phys. Rev. B 71, 205108
- [45] Alicki I and Lieb E, "A proof of part of Haldane's conjecture on spin chains," 1986 Lett. Math. Phys. 12, 57
- [46] Bouwknegt P and Schoutens K, "Exclusion statistics in conformal field theory { generalized fermions and spinons for level-1 WZW theories," 1999 Nucl. Phys. B 547, 501
- [47] Haldane F D M, "Exact Jastrow-Gutzwiller resonating valence bond ground state of the spin-1=2 antiferromagnetic Heisenberg chain with $1/r^2$ exchange," 1988 Phys. Rev. Lett. 60, 635
- [48] Shastri B S, "Exact solution of an $S = 1/2$ Heisenberg antiferromagnetic chain with long-ranged interactions," 1988 Phys. Rev. Lett. 60, 639
- [49] Haldane F D M, "Spontaneous dimerization in the $S = 1/2$ Heisenberg antiferromagnetic chain with competing interactions," 1982 Phys. Rev. B 25, 4925
- [50] Gebhard F and Vollhardt D, "Correlation functions for Hubbard-type models: The exact results for the Gutzwiller wave function in one dimension," 1987 Phys. Rev. Lett. 59, 1472
- [51] Gebhard F and Vollhardt D, "Correlation functions for interacting fermions in the Gutzwiller ansatz," 1988 Phys. Rev. B 38, 6911
- [52] Trivedi N and Ceperley D M, "Green-function Monte Carlo study of quantum antiferromagnets," 1989 Phys. Rev. B (Rapid Comm.) 40, 2737
- [53] Trivedi N and Ceperley D M, "Ground-state correlations in quantum antiferromagnets: A Green-function Monte Carlo study," 1990 Phys. Rev. B 41, 4552
- [54] Read N and Sachdev S, "Valence-bond and spin-Peierls ground states of low-dimensional quantum antiferromagnets," 1989 Phys. Rev. Lett. 62, 1694
- [55] Read N and Sachdev S, "Spin-Peierls, valence-bond solid, and Neel ground states of low-dimensional quantum antiferromagnets," 1990 Phys. Rev. B 42, 4568
- [56] Harada K, Kawashima N and Troyer M, "Neel and spin-Peierls ground states of two-dimensional SU(N) quantum antiferromagnets," 2003 Phys. Rev. Lett. 90, 117203